Potential for Atmospheric-Driven Lead Paint Degradation in the South Coast Air Basin of California

ALEXANDER J. COHAN. RUFUS D. EDWARDS, *, * MICHAEL T. KLEINMAN, § AND DONALD DABDUB

Department of Mechanical & Aerospace Engineering, University of California at Irvine, California 92697-3975, Department of Epidemiology, School of Medicine, University of California at Irvine, California 92697-3957, and Division of Community and Environmental Medicine, School of Medicine, University of California at Irvine, California 92697-1825

Received May 6, 2009. Revised manuscript received September 27, 2009. Accepted October 8, 2009.

Exposure to lead in paint or lead residues in house dust and soil is one of the leading environmental risks to the health of children in the United States. Components of photochemical smog can increase the degradation of binders in lead paint, leading to increased release of lead pigment granules to hands in surface contact or for deposition in house dust and soil. This study uses photochemical air quality modeling to map areas susceptible to increased lead paint degradation as a result of photochemical atmospheric pollutants to prioritize areas of concern. Typical air quality episodes in the South Coast Air Basin of California (SoCAB) are modeled for the 1970s, 1980s, and 1990s. Results indicate that large areas of the SoCAB were susceptible to atmospheric-driven accelerated lead paint degradation. Inner city urban areas from central Los Angeles to Azusa and most of Orange County had the highest susceptibility to accelerated lead paint degradation, followed by inland locations near the San Bernardino Mountains. This study identifies photochemical oxidant gases as contributors to greater lead release from indoor painted surfaces in urban areas.

Introduction

Childhood lead exposure can lead to a number of adverse health effects, including I.O. loss, mental retardation, gastrointestinal pain, visual system deficits, impaired hearing, anemia, lethargy, and in rare cases death (1). Children are more susceptible to lead because they absorb lead to a greater degree than adults and because lead disrupts normal development. Lead exposure has long-term health effects because it is retained in the body for long periods of time, mainly by absorbing into the skeletal system, and can continue to exchange with systemic circulation (1). With the removal of lead from gasoline, the most common pathway of lead exposure for children is from lead-containing dust and physical contact with lead from deteriorated painted surfaces (2, 3).

Although the U.S Product Safety Commission publicly recognized the inherent health risks of lead paint and banned the use of paint containing more than 0.06% lead in 1978 (4), approximately 24 million homes in the United States contain lead-painted surfaces that still pose a serious health concern (5). In addition, that lead paint is still manufactured and used in other nations of the world is of great concern for the health of children globally (6, 7). Lead-based paint is the most commonly cited source of elevated soil lead. Soil collected near foundations of residences contain higher lead concentrations than soil collected at remote locations, indicating deteriorating lead-based paint may primarily supply soils immediately adjacent to the painted surface (8).

A recent study (9) has shown that ozone (O_3) and nitrogen dioxide (NO₂) from photochemical smog increase the degradation of lead-containing paints and accelerates the release of lead to the environment. In the current paper, experimental data from ref 9 are combined with state-of-the-art photochemical air quality modeling to map areas susceptible to increased lead paint degradation as a result of elevated ambient air concentrations of photochemical oxidants in the South Coast Air Basin of California (SoCAB) between the 1970s and 1990s. Given limited resources, this study is a first step in prioritizing areas of concern for residential risk assessments or blood lead testing by evaluating the potential for urban air pollution to increase risks of exposure to lead from lead-based paints in the SoCAB.

Methods

Air Quality in Southern California. Air quality in southern California has improved steadily from 1970 due to aggressive implementation of air quality regulations by the State of California and the U.S. government through the Clean Air Act (CAA) and its amendments. Despite these efforts, air quality in some parts of the SoCAB is among the worst in the United States with respect to photochemical oxidants and particulate matter (PM) due to a number of geographic and meteorological factors. The San Gabriel and San Bernardino Mountains form a natural barrier that enhances accumulation of air pollutants in downwind locations like Riverside and San Bernardino, while coastal winds keep air along the coast relatively clean. In addition, high population density and pollutant emissions in the area cause strong diurnal and weekly variations in air quality.

Model Description. This study uses the University of California Irvine-California Institute of Technology (UCI-CIT) regional photochemical model (10) to assess typical air quality episodes of SoCAB during the 1970s, 1980s, and 1990s. The UCI-CIT model is a comprehensive threedimensional chemical transport model that solves the coupled convection, diffusion, and chemical reaction (eq 1).

$$\frac{\partial C_i}{\partial t} + u \times \nabla C_i = \nabla \times C_i (K \nabla C_i) + R_i(C, t, T) + E_i(x, t) - S_i(x, t) \quad (1)$$

where C_i is the concentration of species i, t is time, u is the wind velocity vector, K is the eddy diffusivity tensor, T is temperature, E and S represent the emissions and removal fluxes of species, respectively, and R is the net chemical production or loss. Equation 1 is solved numerically using operator splitting techniques for gaseous and aerosol phase species, although only gaseous species are considered here. A full description of the numerical implementation employed in the UCI-CIT model is presented in ref 10. Chemical sinks and sources are accounted for with the CalTech Atmospheric

^{*} Corresponding author e-mail: edwardsr@uci.edu; phone: 949-824-4731; address: 101 Theory, Suite 250, Room 258, Irvine, CA 92697-

[†] Department of Mechanical & Aerospace Engineering.

[‡] Department of Epidemiology, School of Medicine.

[§] Division of Community and Environmental Medicine, School of Medicine.

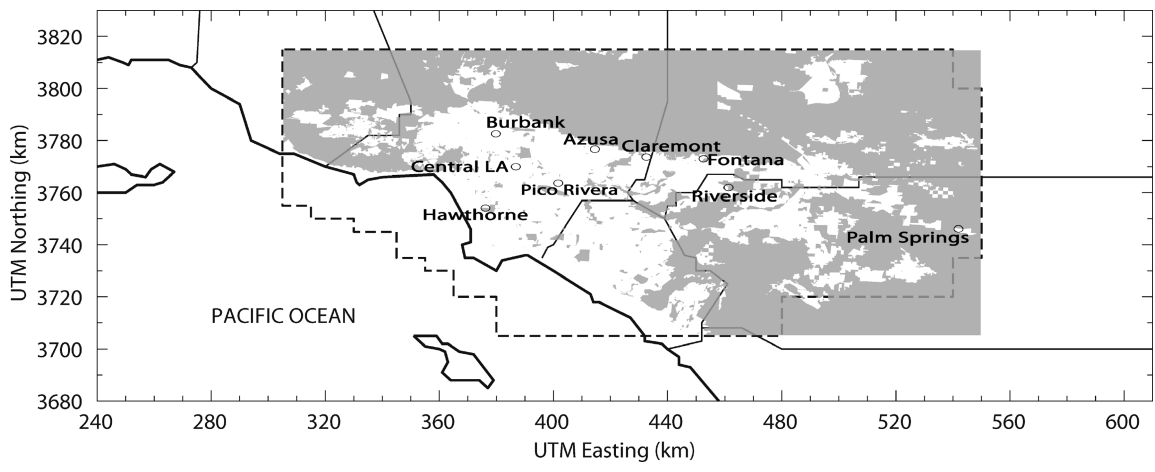


FIGURE 1. Computational domain of the UCI-CIT model is shown with the dashed line. County boundaries are shown with solid lines. Gray areas indicate land undeveloped by 1979 according to 2000 U.S. census block data.

Chemistry Mechanism (CACM), modified to include sea salt-activated chlorine chemistry (11) and modest renoxification (12). Renoxification accounts for the process of deposited NO_X re-entering the atmosphere through surface reactions.

The computational domain, within the dashed lines in Figure 1, contains a large portion of the SoCAB. The computational domain is reduced to examine only properties developed before the banning of leaded paint or within its phasing out period. Historical land use and development for southern California based on 2000 census block data (13) is used to filter out locations developed after 1979 as shown in Figure 1 with gray highlighted areas.

The SoCAB area is typically convection dominated with ocean-driven wind currents running west to east. The computational domain is comprised of 994 cells with a 5 km \times 5 km surface area. The domain extends 1100 m in height and is split into five irregular layers, although here we focus on concentrations of NO₂ and O₃ at ground level.

For each decade of interest, the model simulates a three day Thursday through Saturday episode to account for typical weekday and weekend variations in emission patterns and diurnal peak concentrations (14). This and many other modeling efforts have focused on simulations of several days duration, which is a typical time scale for individual peak O_3 episodes (15). Modeling a short period allows for a more comprehensive treatment of chemical and aerosol processes, which results in a more robust model that will accurately represent the air quality for each decade of interest. Cohan et al. (16) used the UCI-CIT model to predict a similar three day episode and found predicted weekly and diurnal variations compared well with observations.

The UCI-CIT model requires many different types of inputs, including meteorology, chemistry parameters, diffusion coefficients, emissions inventories, and boundary conditions. While many of these parameters are unchanged for all of the simulations investigated, emissions and boundary conditions need to be adjusted to account for shifts in the decades from the 1970s through the 1990s.

Because the largest errors in photochemical modeling are still thought to arise from the meteorological and emission inputs to the model (17), the UCI-CIT model includes area and point emissions, requiring a comprehensive emissions inventory of the SoCAB. The emissions inventory used in this study for the UCI-CIT model is based on measurements obtained August 3–7, 1997, which have been used in the 2003 SoCAB Air Quality Management Plan. Data has been obtained directly from the South Coast Air Quality Management District of California. The emissions inventory includes both weekday and weekend emissions. Boundary conditions

are based on the Southern California Air Quality Study (SCAQS) (18) conducted on August 27–29, 1987.

Boundary conditions and emission inventories are modified for each decade with scaling factors based on total county emissions publicly available from the California Air Resource Board (CARB) (16). Scaling factors generated for each county are separated into four categories by chemical species: oxides of nitrogen, oxides of sulfur, carbon monoxide, and total organic gases. The $\rm O_3$ boundary condition scaling is based on observed yearly maximum $\rm O_3$ concentrations in SoCAB also available from CARB (19).

Additionally, the peroxyacetyl nitrate (PAN) boundary condition is modified slightly for the 1970s simulations. Unlike other boundary conditions, the PAN boundary condition is set to a constant proportion of the $\rm O_3$ concentration at that boundary point. The scaling factor used to determine the PAN boundary concentration is calibrated with data used in the 1980s simulations and shows reasonable agreement when applied to the 1990s data. For the 1970s projected data, the scaling factor is doubled so the PAN boundary concentrations are within an order of magnitude of the concentrations reported by Grosjean (20).

Two different meteorological episodes are examined in this study to determine the sensitivity of results to meteorology. The meteorology prevalent during the SCAQS study is representative of SoCAB (21); this episode represents average meteorological conditions in SoCAB that are not considered intense or weak. The meteorological conditions during the SCAQS study of August 27–29, 1987, are characterized by a weak onshore pressure gradient and warming temperatures aloft. The wind flow is characterized by a sea breeze during the day and a weak land—mountain breeze at night. The presence of a well-defined diurnal inversion layer at the top of neutral and unstable layers near the surface, along with a slightly stable nocturnal boundary layer, facilitated the accumulation of pollutants over the SoCAB and led to the development of high O₃ concentrations in the region.

An alternative meteorological episode observed September 9, 1993, was previously studied (22) to validate the CACM mechanism. The 1993 meteorological episode is more intense than the SCAQS 1987 meteorological episode and provides a worst case air pollution scenario. The September 9, 1993, episode is characterized by slow winds and slightly higher temperatures than the SCAQS episode. In addition, the direction of the wind is predominantly toward the eastern desert. These conditions resulted in some of the highest O₃ concentrations observed in 1993.

The 1993 episode will herein be referred to as the intense meteorological case, and the SCAQS 1987 meteorological

episode will herein be referred to as the average meteorological case. Each decade scenario is run with the intense and average meteorology episodes to examine the influence of meteorology on results.

Lead Paint Degradation. Edwards et al. (9) measured the lead availability of surfaces painted with low gloss solvent lead paint exposed to O_3 and NO_2 in stainless steel chambers, using the modified NIOSH wipe method 9100 and analysis method 7105. Lead paint degrades faster in the presence of typical atmospheric pollutants and therefore can increase the amount of lead made available to the environment from painted surfaces containing lead (9).

In the above study (9), O_3 and NO_2 consumption in chambers remained constant over the course of the experiment; therefore, empirical constants α_1 and α_2 were derived to relate the increase in the mass of additional available lead to the time integrated exposure concentration of O_3 and NO_2 , respectively. These constants are expressed in terms of additional lead mass per area ($\alpha_1 = 1.32 \times 10^{-8}~\mu g~cm^{-2}~ppb^{-1}~h^{-1}$ and $\alpha_2 = 12.32 \times 10^{-8}~\mu g~cm^{-2}~ppb^{-1}~h^{-1}$) and in terms of percent increase of lead mass per area ($\alpha_1 = 1.85 \pm 1.11 \times 10^{-5}~\%~ppb^{-1}~h^{-1}$). Lead availability is more sensitive to NO_2 than O_2 exposure

The empirical constants are used to relate the pollutiondriven lead paint degradation increase or lead availability, LA, to the time integrated O₃ concentration, IO₃, and time integrated NO₂ concentration, INO₂ (eq 2).

$$LA = \alpha_1 IO_3 + \alpha_2 INO_2 \tag{2}$$

where ${\rm IO_3}$ and ${\rm INO_2}$ are in units of ppb hr and LA is in units of % or $\mu {\rm g/cm^2}$, depending on the empirical constants. The time integrated concentration is approximated with a Riemann sum of 1 h average concentrations at each ground level grid node. Equation 2 allows the calculation of the acceleration in lead availability to the environment from a painted surface area caused by an atmospheric episode. While the laboratory study (9) only reported the response of lead paint to individual pollutants, their results are superimposed in eq 2. Preliminary chamber experiments examining the combined effect of ${\rm O_3}$ and ${\rm NO_2}$ indicate that the superposition presented in eq 2 under-predicts observations.

Equation 2 is used to predict the influence of atmospheric conditions on lead paint degradation over a monthly and annual period. The modeled three day episode is used to scale $\rm O_3$ and $\rm NO_2$ concentrations over a four week period for each decade from the 1970s through 1990s to approximate a monthly integrated exposure episode. The predicted $\rm O_3$ and $\rm NO_2$ profiles for Thursday and Friday are used 10 times each, and the Saturday profile is used 8 times, for a total of 28 days. Monthly exposures are calculated for intense and average meteorological episodes to examine the meteorological variability.

Winner and Cass (23) evaluated the annual frequency distribution of O_3 for 1987 in southern California. In the Los Angeles basin, 8 h peak O_3 concentrations exceeded 120 ppb 37.2% of the time depending on meteorology. Because ozone episodes occur throughout the year in Los Angeles (19), to estimate annual increases in lead paint degradation, 37.2% of the year was characterized as intense air quality episodes, with the remainder composed of average air quality.

The normalized error can be propagated from eq 2 with standard error analysis (24) to account for model and empirical error.

$$\partial LA = \sqrt{\left(\partial \alpha_1\right)^2 + \left(\partial \alpha_2\right)^2 + \left(\partial O_3\right)^2 + \left(\partial NO_2\right)^2} \tag{3}$$

where ∂ indicates the normalized or fractional uncertainty. Using a similar regional photochemical model with daily

peak 1 h O_3 concentrations of similar magnitude as the current model, Harley et al. (15) reported the normalized errors for O_3 and NO_2 as 23% and 17%, respectively. Overall uncertainty in modeled lead paint degradation rates was $\pm 75\%$, with 53% attributable to uncertainty from wipe tests of lead painted surfaces and 22% from uncertainty in modeled atmospheric oxidant concentrations. Because uncertainty from wipe tests of lead painted surfaces was largely dominated by variability in wipe procedures rather than lead release rates (9), overall uncertainty estimates likely overestimate uncertainty in lead paint degradation rates.

Another empirical approach is to examine the time derivative of eq 2

$$LAR = \alpha_1 O_3 + \alpha_2 NO_2 \tag{4}$$

where LAR is the lead availability rate in units of $\% h^{-1}$, O_3 is the O_3 concentration in ppb, and NO_2 is the NO_2 concentration in ppb. The lead availability rate is the flux of lead availability relative to time. Equation 4 is used to relate directly O_3 and NO_2 concentrations to the rate of lead made available from lead paint at any moment and location.

Equation 2 is used to create a risk map of lead availability derived from paint degradation, which offers insight into the overall effect of pollution-driven lead paint degradation, while also accounting for diurnal, weekend versus weekday, and meteorological variations in lead paint degradation as a result of variability in atmospheric photochemistry. Because of the considerable uncertainties in paint application in homes and other sources of lead exposure, the risk maps are intended as engineering insight to prioritize areas of concern as a result of this mechanism as opposed to estimating absolute concentrations for personal exposure estimates.

Results

Figure 2 shows the increase in degradation of lead-painted surfaces as a result of exposure to ambient O_3 and NO_2 over a four week period for areas built prior to the ban on lead-based paints in 1978. Figure 2 follows the general trend of air quality in SoCAB. Locations with large NO_2 emissions sources such as downtown Los Angeles and Riverside show the highest lead availability. Lead availability down wind, in places like Palm Springs, is more sensitive to O_3 formation because of deposition and transformation of NO_2 . The San Bernardino Mountains form a natural eastern border that traps air parcels, causing accumulation of O_3 to the east. The intense meteorology produces higher lead availability than the average meteorology, which is reflected in the lead availability contours.

Table I shows annual increases in lead release from lead-based paints for the cities labeled in Figure 2 in terms of additional mass of lead release and percent increase of lead release. Azusa and downtown Los Angeles show the highest increases in lead release from paint degradation, while Palm Springs is least affected. Additionally, Los Angeles, Pico Rivera, and Azusa were more developed by 1979 than Palm Springs, as illustrated in Figures 1 and 2. The annual potential lead availability from degraded paint in downtown Los Angeles is over twice as much as that in Palm Springs for every modeled decade, indicating significant spatial variability from the influence of pollutants on lead paint degradation.

The lead availability produced from a monthly integrated O_3 and NO_2 exposure episode is shown in Figure 3 at select cities within the SoCAB under normal and intense meteorology months during the different decades. There has been considerable improvement in air quality from the 1970s through 1990s in the SoCAB because of strong emission standards and regulations. Lead paint degradation rates under intense meteorology show a decrease in paint degradation caused by atmospheric pollution from the 1970s to

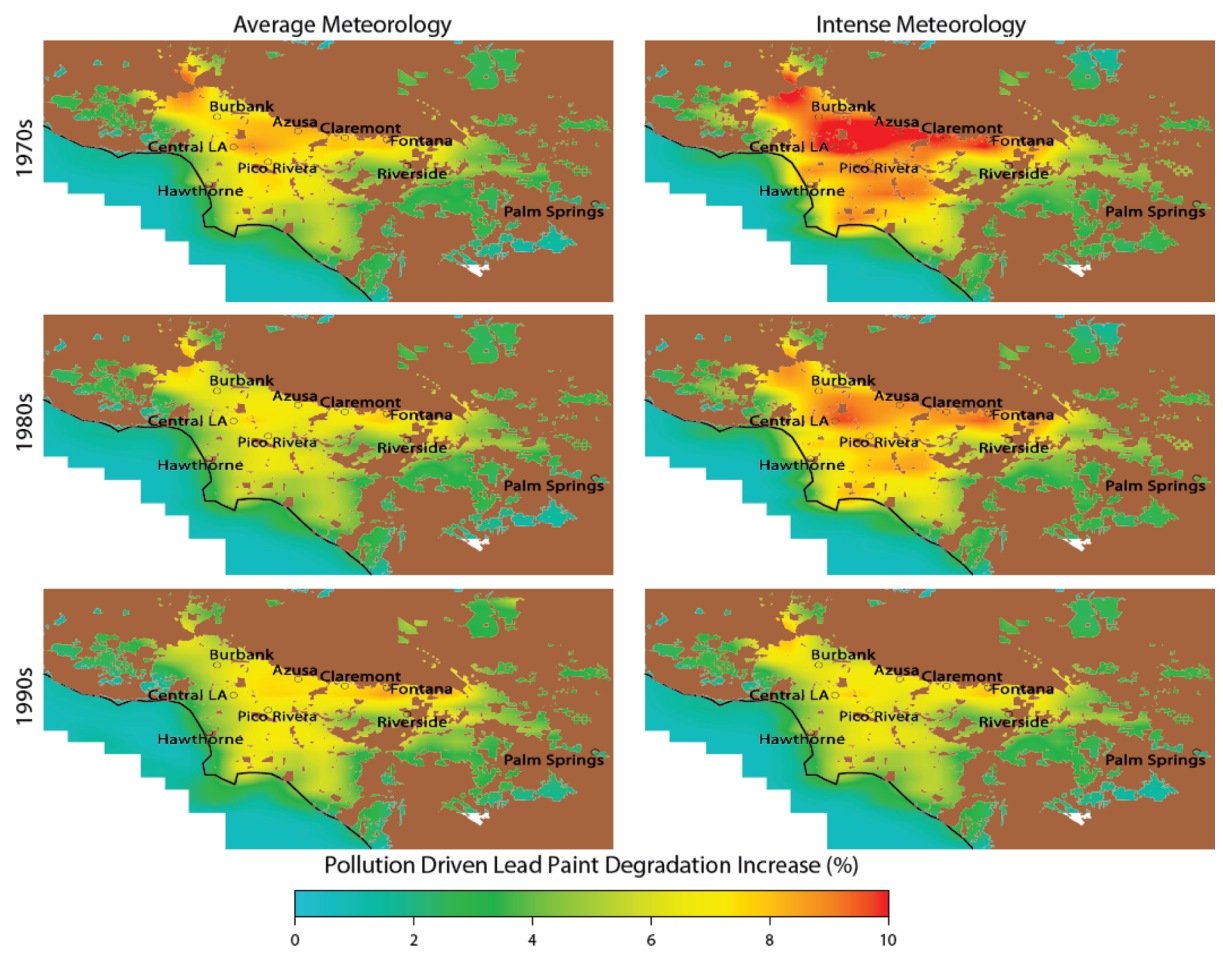


FIGURE 2. Predicted pollution-driven lead paint degradation increase (%) caused by monthly integrated $\mathbf{0}_3$ and $\mathbf{N0}_2$ exposure over the South Coast Air Basin of California. Simulations of 1970s, 1980s, and 1990s are shown from top to bottom, respectively. An average meteorology case is shown on the left, while an intense meteorology case is shown on the right. Brown areas indicate land undeveloped by 1979 according to 2000 U.S. census block data.

TABLE 1. Pollution-Driven Lead Paint Degradation Increase by Mass and Percent Mass Caused by an Average Annual Atmospheric Episode for Cities in the South Coast Air Basin of California

| | | $10^{-2}~\mu\mathrm{g/cm^2}$ | | | % | | |
|---------------|------|------------------------------|-------|-------|-------|-------|-------|
| city | ABR | 1970s | 1980s | 1990s | 1970s | 1980s | 1990s |
| Burbank | BURK | 8.4 | 7.1 | 7.0 | 104 | 89 | 79 |
| L.A. downtown | CELA | 9.7 | 8.4 | 8.4 | 120 | 104 | 91 |
| Pico Rivera | PICO | 8.4 | 7.4 | 7.5 | 104 | 92 | 87 |
| Hawthorne | HAWT | 8.0 | 7.1 | 4.0 | 99 | 87 | 58 |
| Azusa | AZUS | 10.2 | 8.5 | 9.2 | 127 | 106 | 101 |
| Claremont | CLAR | 8.4 | 7.7 | 8.3 | 105 | 97 | 96 |
| Fontana | FONT | 9.0 | 8.7 | 9.5 | 113 | 109 | 107 |
| Riverside | RIVR | 6.3 | 6.5 | 5.8 | 80 | 82 | 74 |
| Palm Springs | PLSP | 3.0 | 3.1 | 3.3 | 42 | 43 | 35 |

1990s, except for Riverside and Palm Springs, which were slower to develop. Under average meteorology, reductions in lead degradation rates across decades are much less than that observed under intense meteorology. In addition, lead degradation rates are similar in the 1980s and 1990s, which is the result of increased photochemical production of O_3 in the 90s, despite decreases in NO_χ emissions due to a nonlinear relationship with local volatile organic compounds and oxides of nitrogen (25).

Table 2 summarizes the results of analyzing the daily lead availability rates in central Los Angeles, Palm Springs, and Riverside on weekdays and weekends under average and intense meteorology. Degradation rates are largely influenced by location and local photochemistry. For example, lead paint degradation rates under intense meteorology are not significantly reduced between decades on weekends in Palm Springs and Riverside but are reduced on weekdays. The difference between weekday and weekend arises as a result of the well-observed phenomenon of increased $\rm O_3$ production during the weekend despite a decrease in total emissions compared to weekdays (26). In contrast, lead paint degradation rates in Los Angeles are relatively similar throughout the decades on weekdays and weekends, resulting in greater overall lead paint degradation, largely driven by $\rm NO_2$ emissions from traffic.

Discussion

This study is the first step in mapping the potential for typical local air quality to increase lead paint degradation in the SoCAB from the 1970s through 1990s and prioritizes areas of potential concern in older housing stock. The SoCAB has transformed significantly from the 1970s to 1990s with changes in land use, population, and anthropogenic emissions all affecting lead availability calculations. Figure 1 shows the superposition of historical census tract housing from the 1970s within the areas of potentially increased atmospheric-driven lead paint degradation. The 2000 census block data of historical progression of development in California (13) identifies specific areas that had not been developed by 1979, highlighted in gray in Figure 1. This data allows our study to focus on regions that could have used leaded paint in their development.

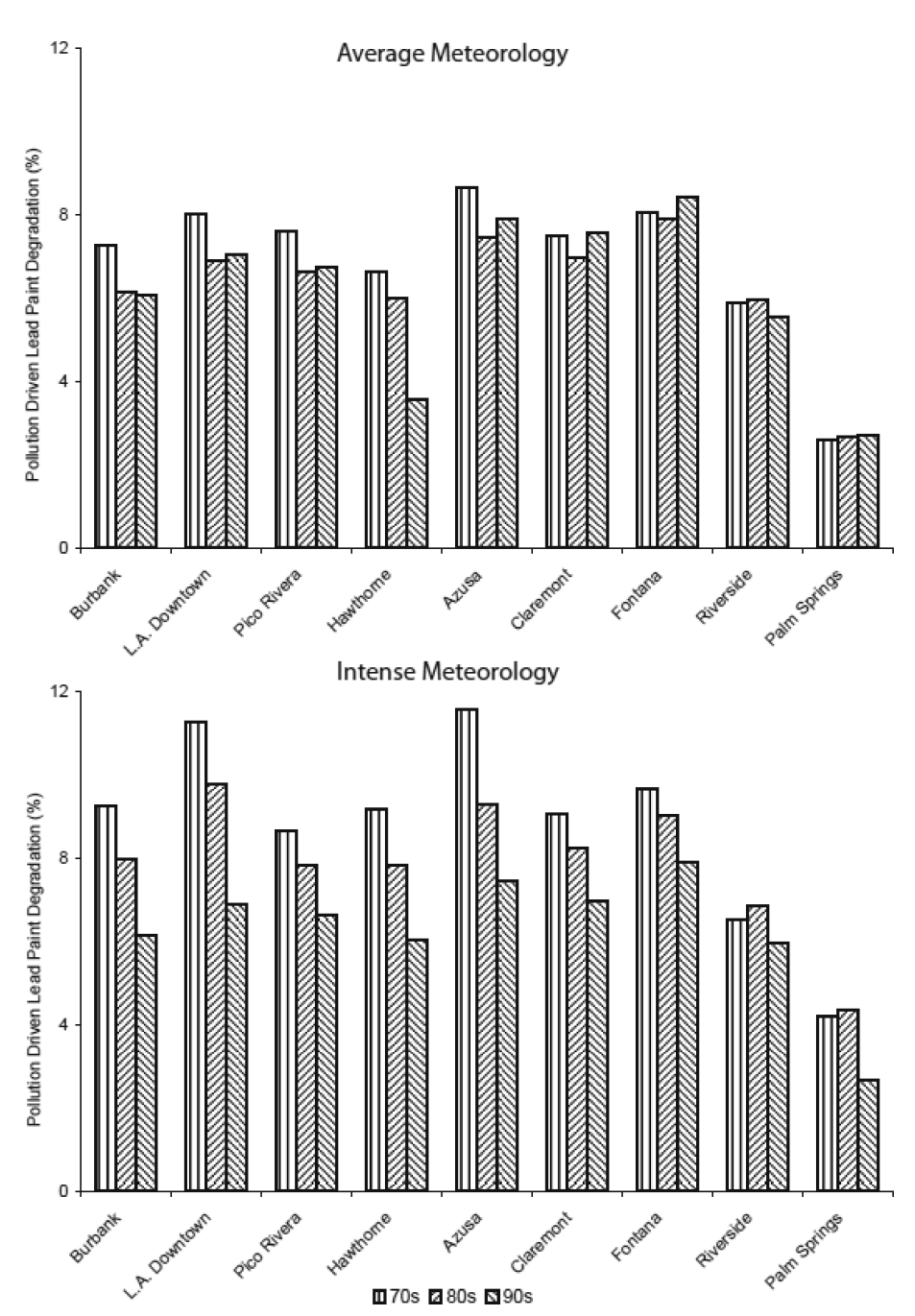


FIGURE 3. Pollution-driven lead paint degradation increase (%) caused by monthly integrated O_3 and NO_2 exposure at cities within the South Coast Air Basin of California. Average and intense meteorology scenario results are shown on top and bottom, respectively.

Los Angeles has strong nitrogen emissions and O₃ production, making it more susceptible to lead paint degradation. The lead availability contours generally show a decrease in the lead paint degradation rates from the 1970s through 1990s. The areas of highest lead exposure risk extend from Los Angeles to Riverside, where there are high concentrations of O₃ and NO₂. Azusa and Fontana are statistically within the top 2% of one month integrated lead availability from pollution-driven paint degradation over the entire SoCAB domain. The eastern side of the domain has relatively good air quality with little pollution and a small change in air quality between the 1970s through 1990s. Hence, the eastern low-risk areas tend to see a minor improvement in lead availability from the 1970s through 1990s, while the western high-risk areas see a more dramatic decrease in lead availability from the 1970s through 1990s.

Palm Springs and Riverside are two of the lowest risk cities in SoCAB for all three periods examined, with little total change in lead availability from painted surfaces. These areas are downwind of the large NO_X emissions, where photochemistry and transport increase O_3 production. The impact of O_3 production on lead paint degradation is reduced, however, compared with the stronger correlated degradation caused by NO_2 . Thus, the lead availability contour plots shown in Figure 2 more closely resemble 24 h average NO_2 contours than 24 h average O_3 contours, which is concurrent with the empirical relations applied.

There is very little information about factors affecting degradation rates of lead-based paints. A variety of household factors may be sources of variability in lead paint degradation such as type and formulation of paint use, thickness of coating, paint application type, physical abrasion, and

TABLE 2. Summary of Daily Predictions of Pollution-Driven Lead Paint Degradation Rates caused by O_3 and NO_2 Exposure at Select Locations across the South Coast Air Basin of California

| 1 h daily average | (+ standard deviation |) lead availability rate | (10-3 % h-1) |
|--------------------|------------------------|--------------------------|-------------------|
| i ii uaiiv aveiaue | t = Standard deviation | ı) iedu avanapınıv rale | : (IU - 70 II ·) |

| | | average meteorology | | intense meteorology | | |
|--------------|-------|---------------------|----------------------------------|----------------------------------|---------------------------------|--|
| | | weekday | weekend day | weekday | weekend day | |
| Los Angeles | 1970s | 10.6 ± 2.6 | $\textbf{10.8} \pm \textbf{1.4}$ | $\textbf{15.1} \pm \textbf{6.0}$ | 15.7 ± 2.4 | |
| | 1980s | 9.9 ± 2.2 | 9.8 ± 1.3 | 14.0 ± 5.6 | 13.9 ± 2.3 | |
| | 1990s | 10.0 ± 2.8 | 10.1 ± 2.9 | $\textbf{13.4} \pm \textbf{4.1}$ | 14.3 ± 5.5 | |
| Palm Springs | 1970s | 10.6 ± 1.5 | 3.5 ± 0.8 | 15.1 ± 1.0 | 7.1 ± 3.0 | |
| | 1980s | 4.5 ± 1.3 | 3.6 ± 0.7 | 6.0 ± 1.0 | 7.1 ± 2.4 | |
| | 1990s | 3.9 ± 1.2 | 4.0 ± 1.0 | 5.9 ± 1.5 | $\textbf{9.2} \pm \textbf{2.3}$ | |
| Riverside | 1970s | 10.6 ± 3.0 | 6.4 ± 2.8 | 15.1 ± 3.4 | 9.6 ± 3.9 | |
| | 1980s | 9.0 ± 2.5 | 8.9 ± 5.1 | 8.8 ± 3.3 | 10.8 ± 5.5 | |
| | 1990s | 9.8 ± 2.6 | 6.3 ± 2.7 | 9.6 ± 1.7 | 8.1 ± 2.9 | |

cleaning. However, these sources of variability would be expected to be more randomly distributed spatially among communities within Los Angeles. The current paper addresses the spatial context of lead availability among communities as a result of the reaction of oxidant gases. The results of this modeling study are intended as a tool that may be used to target efforts to evaluate blood lead levels and residential risk assessments or inform pediatricians of the need for blood lead testing, given the high prevalence of homes in Los Angeles with lead-based paint. Finally, understanding the spatial patterns of lead paint degradation may help in relating X-ray fluorescence measurements of lead present in lead-based paint in homes as part of risk assessments of blood lead levels in children.

Air quality models have inherent uncertainty from discretization, truncation, and input parameters, in addition to variability in lead paint degradation rates from laboratory measurements (9). The numerical uncertainties from O₃ and NO₂ are some of the smallest compared with organic compounds or PM. On average, the UCI-CIT model using a similar chemical mechanism, has been shown to produce peak O₃ concentrations that are within 23% of observational peaks (27, 15). The lead availability relationship with atmospheric pollutants only considers O₃ and NO₂ and serves as a lower bound estimate of the potential lead made available through pollution-driven lead paint degradation for normal indoor leaded paint. There are many more caustic and harmful air pollutants that are yet unaccounted for as well as additional degradation from nonlinear combined effects of multiple pollutants. However, O₃ and NO₂ do represent two of the most abundant chemical species represented in CACM. In addition, the current modeling reflects the degradation of one lead-based paint formulation. There are many different paint formulations, however, that may be more or less affected by O₃ and NO₂, which are not reflected in the current models largely because of the difficulties in evaluating which paint formulations were applied in specific locations. Thus, these models only reflect the potential for increased atmospheric lead paint degradation rather than exposure risk.

Additional uncertainties arising from model predictions can be seen in the differences between average and intense meteorology as well as the variability of predictions across SoCAB. Propagated uncertainty is estimated at 75% for data shown in Figures 2 and 3 and Table 1, with the majority of the uncertainty related to the lead wipe test (9).

Although a principal source of high blood lead levels (8), lead from painted surfaces represents only one lead exposure factor. Because of historical impacts of lead emissions from the use of lead as a gasoline additive, soil in downtown Los

Angeles has high levels of residual lead contamination (28) that continues to be a source of lead exposure to children and adults from direct hand-to-mouth contact and inhalation of resuspended particulate matter. In addition to evaluating the paint coverage in individual homes, incorporation of historic traffic and other potential sources of lead would be required to derive maps related to lead exposure or blood lead levels.

Atmospheric-driven lead paint degradation is presented under both meteorological scenarios. The intense meteorology produces an increase in lead availability for the high-risk areas of Azusa, Fontana, and downtown Los Angeles, and a small increase or no change in lead availability for the lowrisk areas of Palm Springs, Riverside, and Hawthorne compared with the average meteorology. On average, the intense meteorology produces 8% more lead availability than the average meteorology. Although results identify a decrease in the potential for atmospheric lead paint degradation between the 1970s and 1990s, actual atmospheric lead degradation rates would decline much more rapidly reflecting the sequential covering of lead-painted surfaces as household surfaces were repainted, if such measurements were taken. Although O₃ and NO₂ would act to increase the degradation rates of the paint coverings, increasing the chances of peeling, cracking, and splitting, these would not occur for a considerable period after the surfaces had been repainted.

Results show a large range of potential increases in lead availability by location in SoCAB with a maximum of 12.5% and minimum 5 orders of magnitude lower over a one month period. There is no known safe level of lead in blood, especially for children (29), and the quantitative relationship between increased lead availability from lead-based paints and blood lead levels is unknown. However, increased availability of lead residues from painted surfaces would be expected to cause increases in blood lead levels in children with similar activity patterns and lead sources in the home and may be a factor in explaining the higher rates of lead poisoning in urban areas.

Finally, these results demonstrate the interaction and superposition of environmental risk factors in urban areas as areas with poor air quality amplify the additional health concern of lead paint degradation in addition to health impacts of poor air quality itself. This is of particular concern for low-income inner city neighborhoods that would be expected to repaint less frequently and may be a factor in the increased lead poisoning in marginalized populations (5).

Acknowledgments

This study was conducted at the University of California, Irvine, in the computational environmental science (CES) laboratory. Funding for this project was provided by a grant from the U.S. Department of Housing and Urban Development (CALHT0108-04 to R.D.E.)

Literature Cited

- Bostrom, A. Lead is like mercury: Risks comparisons, analogies, and mental models. J. Risk Res. 2008, 11 (1), 99–117.
- (2) Dixon, S. Selecting a lead hazard control strategy based on dust lead loading and housing condition: I. Methods and results. J. Occup. Environ. Hyg. 2008, 5 (8), 530–539.
- (3) Jacobs, D. E. Lead-Based Paint as a Major Source of Childhood Lead Poisoning: A Review of the Evidence. In Lead in Paint, Soil, and Dust: Health Risks, Exposure, Control Measures, Measurement Methods, and Quality Assurance. ASTMP STP 1226. Beard, M., Allen Isk, S. D., Eds.; American Society for Testing and Materials, West Conshohocken, PA, 1995; pp 175–189.
- (4) Management and Disposal of Lead-Based Paint Debris; Proposed Rule. Federal Register, CFR 63; United States Environmental Protection Agency: Washington, DC, 1998; Volume 63, Number 243, pp 70190-70233.
- (5) Meyer, P. A.; Brown, M. J.; Falk, H. Global approach to reducing lead exposure and poisoning: Mutation research. *Mutat. Res.* **2008**, 659 (1–2), 166–175.
- (6) Clark, C. S.; Rampal, K. G.; Thuppil, V. G.; Chen, C. K.; Clark, R.; Roda, S. The lead content of currently available new residential paint in several Asian countries. *Environ. Res.* 2006, 102 (1), 9–12.
- (7) Lin, G. Z.; Preng, R. F.; Chen, Q.; Wu, Z. G.; Du, L. Lead in housing paints: An exposure source still not taken seriously for children lead poisoning in China. *Environ. Res.* 2009, 109 (1), 1–5.
- (8) Burgoon, D. A.; Brown, S. F.; Menton, R. G. Literature Review of Sources of Elevated Soil—Lead Concentrations. In Lead in Paint, Soil, and Dust: Health Risks, Exposure, Control Measures, Measurement Methods, and Quality Assurance. ASTMP STP 1226. Beard, M., Allen Isk, S. D., Eds.; American Society for Testing and Materials, West Conshohocken, PA, 1995; pp 76–91.
- (9) Edwards, R. D.; Lam, N.; Zhang, L.; Johnson M. J.; Kleinman M. T. NO₂ and ozone as factors in the availability of lead from lead-based paints. *Environ. Sci. Technol.*, 2009, in press.
- (10) Dabdub, D.; Seinfeld, J. H. Numerical advective schemes used in air quality models: Sequential and parallel implementation. *Atmos. Environ.* **1994**, *28* (20), 3369–3385.
- (11) Knipping, E. M.; Dabdub, D. Impact of chlorine emissions from sea salt aerosol on coastal urban ozone. *Environ. Sci. Technol.* 2003, 37 (2), 275–284.
- (12) Knipping, E. M.; Dabdub, D. Modeling surface-mediated renoxification of the atmosphere via reaction of gaseous nitric oxide with deposited nitric acid. *Atmos. Environ.* 2002, 36, 5741– 5748.
- (13) Development, Historical Progression, 2007. California Department of Forestry and Fire Protection. frap.cdf.ca.gov/data/frapgismaps/select.asp (accessed 2009).

- (14) Winner, D. A.; Cass, G. R. Modeling the long-term frequency distribution of regional ozone concentrations. *Atmos. Environ.* 1999, 33 (3), 431–451.
- (15) Harely, R. A.; Russell, A. G.; McRae, G. J.; Cass, G. R.; Seinfeld, J. H. Photochemical modeling of the southern California air quality study. *Environ. Sci. Technol.* 1993, 27 (2), 378–388.
- (16) Cohan, A.; Chang, W.; Carreras-Sospedra, M.; Dabdub, D. Influence of sea salt-activated chlorine and surface-mediated renoxification on the weekend effect in the South Coast Air Basin of California. Atmos. Environ. 2008, 42 (13), 3115–3129.
- (17) Russel, A.; Dennis, R. NARSTO critical review of photochemical models and modeling. Atmos. Environ. 2000, 34, 2283–2324.
- (18) Lawson, D. The Southern California air quality study. J. Air Waste Manage. Assoc. 1990, 40 (2), 156–165.
- (19) Data and Statistics, 2007. California Air Resource Board. www.arb.ca.gov (accessed 2008).
- (20) Grosjean, D. Ambient PAN and PPN in Southern California from 1960 to the SCOS97-NARSTO. Atmos. Environ. 2003, 37 (2), S221– S238.
- (21) Zeldin, M. D.; Bregman, L. D.; Horie, Y. A meteorological and air quality assessment of the representativeness of the 1987 SCAQS Intensive Days: Final report to the South Coast Air Quality Management District, 1990.
- (22) Griffin, R. J.; Dabdub, D.; Kleeman, M. J.; Fraser, M. P.; Cass, G. R.; Seinfeld, J. H. Secondary organic aerosol. 3. Urban/regional scale model of size- and composition-resolved aerosols. *Journal of Geophysical Research* 2002, 107 (D17), 4334–4347.
- (23) Winner, D. A.; Cass, G. R. Modeling the long-term frequency distribution of regional ozone concentrations. *Atmos. Environ.* 1999, 33 (3), 431–451.
- (24) Taylor, J. R. An Introduction to Error Analysis: The Study of Uncertainties in Physical Measurements; University Science Books: Sausalito, CA, 1997.
- (25) Nguyen, K.; Dabdub, D. NO_X and VOC control and its effect on the formation of aerosols. *Aerosol Sci. Technol.* 2002, 36 (5), 560–572.
- (26) Qin, Y.; Tonnesen, G. S.; Wang, Z. Weekend/weekday differences of ozone, NO_X, CO, VOCs, PM₁₀, and the light scatter during ozone season in southern California. *Atmos. Environ.* **2004**, *38* (19), 3069–3087.
- (27) Harley, A.; Sawyer, R.; Milford, J. Updated photochemical modeling for California's South Coast Air Basin: Comparison of chemical mechanisms and motor vehicle emission inventories. *Environ. Sci. Technol.* 1997, 31 (10), 2829–2839.
- (28) Wu, J.; Klienman, M.; Edwards, R. Spatial analysis of soil lead concentrations in Los Angeles, California, U.S.A. *Epidemiology* **2008**, *19* (6), S157–S157.
- (29) Lanphear, B. P.; Hornung, R.; Khoury, J.; Yolton, K.; Baghurst, P.; Bellinger, D. C.; Canfield, R. L.; Dietrich, K. N.; Bornschein, R.; Greene, T.; Rothenberg, S. J.; Needleman, H. L.; Schnaas, L.; Wasserman, G.; Graziano, J.; Roberts, R. Low-level environmental lead exposure and children's intellectual function: An international pooled analysis. *Environ. Health Perspect.* 2005, 113 (7), 894–899.

ES901360J